International Journal of Modeling, Simulation,
and Scientific Computing
Vol. 8, No. 4 (2017) 1750040 (16 pages)

DOI: 10.1142/S1793962317500404

Mechanical response and simulation for constitutive equations with distributed order derivatives

Jun-Sheng Duan*

School of Sciences, Shanghai Institute of Technology
100 Haiquan Road, Fengxian District, Shanghai 201418, P. R. China
duanjs@sit.edu.cn

YangQuan Chen

MESA Lab, University of California, Merced
5200 North Lake Road, Merced, CA 95343, USA
ychen53@ucmerced.edu

Received 15 November 2016
Accepted 23 February 2017
Published 11 April 2017

Mechanical response and simulation for constitutive equation with distributed order derivatives were considered. We investigated the creep compliance, creep recovery, relaxation modulus, stress–strain behavior under harmonic deformation for each case of two constitutive equations. We express these responses and results as easily computable forms and simulate them by using MATHEMATICA 8. The results involve the exponential integral function, convergent improper integrals on the infinite interval $(0, +\infty)$ and the numerical integral method for the convolution integral. For both equations, stress responses to harmonic deformation display hysteresis phenomena and energy dissipation. The two constitutive equations characterize viscoelastic models of fluid-like and solid-like, respectively.

Keywords: Fractional calculus; constitutive equation; response; distributed order derivative.

1. Introduction

Fractional calculus has been applied to mathematical description of real problems arising in different fields of science and engineering, such as viscoelasticity, anomalous diffusion, control theory, relaxation and oscillation, etc.[1–16] It is capable for describing memory and hereditary properties of various materials and processes. In viscoelasticity theory, fractional calculus has been used to establish constitutive equations conveniently and effectively.[1–8,17–20] The part reasons for the development

*Corresponding author.

of the viscoelasticity theory are the wide use of polymers in various fields of engineering. Also viscoelastic materials are extensively applied to cushion shock, from running shoes to packing materials.

Let $f(t)$ be piecewise continuous on $(0, +\infty)$ and integrable on any finite subinterval of $(0, +\infty)$. Then the Riemann–Liouville fractional integral of $f(t)$ of order β is defined as

$$ {}_0J_t^\beta f(t) = \int_0^t \frac{(t-\tau)^{\beta-1}}{\Gamma(\beta)} f(\tau) d\tau, \quad t > 0, \tag{1} $$

where β is a positive real number, and $\Gamma(\cdot)$ is Euler's gamma function. For complementarity, we define ${}_0J_t^0 f(t) = f(t)$.

Let α be a positive real number satisfying $m - 1 < \alpha \leq m$ and $m \in \mathbb{N}^+$, where $\mathbb{N}^+$ is the set of positive integers. Then the Riemann–Liouville fractional derivative of $f(t)$ of order α is defined, when it exists, as

$$ f^{(\alpha)}(t) = {}_0D_t^\alpha f(t) = \frac{d^m}{dt^m}({}_0J_t^{m-\alpha} f(t)), \quad t > 0. \tag{2} $$

Scott-Blair[1,2] proposed a fractional constitutive equation $\sigma(t) = E\,\epsilon^{(\alpha)}(t)$, where E and α are material-dependent constants and $0 < \alpha < 1$, to characterize a viscoelastic material whose mechanical properties are intermediate between those of a pure elastic solid (Hooke model) and a pure viscous fluid (Newton model). In Refs. 7 and 21, this relation was called as the Scott-Blair model. In Ref. 5, a fractional calculus element whose constitutive law obeys stress is proportional to a fractional derivative of strain is said to be a spring-pot.

Macromolecule polymers such as polybutadiene and butyl are typical viscoelastic material whose constitutive relation may be modeled by using fractional derivatives.[18] Different fractional constitutive equations have been proposed, such as the fractional Maxwell, Kelvin–Voigt, and Zener models by replacing Newton's classical elements by the Scott-Blair element.[17–20,22]

The distributed order derivative and associated equations were proposed in Refs. 23–25. In Refs. 23 and 24, distributed order equations were analyzed by expressing them as equivalent distributed order integral equations. In Ref. 25, distributed order equations were used to model dielectric induction and diffusion.

In Refs. 26 and 27, the following distributed order constitutive equation was proposed

$$ \int_0^1 \phi_\sigma(\alpha)\sigma^{(\alpha)}(t) d\alpha = \int_0^1 \phi_\epsilon(\alpha)\epsilon^{(\alpha)}(t) d\alpha, \tag{3} $$

where $\phi_\sigma(\alpha)$ and $\phi_\epsilon(\alpha)$ are given functions or constitutive functions. In Refs. 28–30, stability, simulation and applications of distributed order systems are discussed. In Eq. (3), the functions $\phi_\sigma(\alpha)$ and $\phi_\epsilon(\alpha)$ assign weights to the order α. So we expect Eq. (3) could be used to describe viscoelastic materials with complex structure.

In this paper, we investigate the response and its modeling for the distributed order constitutive equation (3) for two cases: Case A $\phi_\sigma(\alpha) = \delta(\alpha)$, $\phi_\epsilon(\alpha) = E\ (\tau_0)^\alpha$

and Case B $\phi_\sigma(\alpha) = (\tau_\sigma)^\alpha,\ \phi_\epsilon(\alpha) = E\ (\tau_\epsilon)^\alpha$, where $\delta(\alpha)$ is the Dirac delta function, $E, \tau_0, \tau_\sigma, \tau_\epsilon$ are constants. We demonstrate characteristics of viscoelastic materials such as creep, relaxation, energy dissipation or hysteresis under deformation, etc., by using the distributed order constitutive equation.

The involved functions of a single variable t are of causality requirement, that is, they are vanishing for $t < 0$. The unit step function or the Heaviside function is denoted by $H(t)$.

We use the definition of the Laplace transform of $f(t)$

$$\bar{f}(s) = L[f(t)] = \int_{0^-}^{\infty} f(t)e^{-st}dt, \quad \mathrm{Re}(s) > c, \tag{4}$$

and its inversion formula

$$f(t) = L^{-1}[\bar{f}(s)] = \frac{1}{2\pi i}\int_{\mathrm{Br}} \bar{f}(s)e^{st}\mathrm{d}s, \tag{5}$$

where Br denotes the Bromwich contour, i.e., the straight line from $s = c - i\infty$ to $s = c + i\infty$.

Applying the Laplace transform to Eq. (3), we have

$$\bar{\sigma}(s) = \frac{\int_0^1 \phi_\epsilon(\alpha)s^\alpha d\alpha}{\int_0^1 \phi_\sigma(\alpha)s^\alpha d\alpha}\ \bar{\epsilon}(s). \tag{6}$$

Creep compliance and relaxation modulus are two important material functions describing mechanical characteristics of viscoelastic materials. Creep compliance is the strain response to an instantaneous applied fixed unit stress described by the Heaviside function $\sigma(t) = H(t)$. The relaxation modulus $G(t)$ is the behavior of stress decreasing or relaxing over time under a suddenly applied fixed unit strain $\epsilon(t) = H(t)$. Both the material functions are nonnegative. Furthermore, for $0 < t < +\infty$, $J(t)$ is nondecreasing and $G(t)$ is nonincreasing.

Thus, the Laplace transforms of the creep compliance $J(t)$ and the relaxation modulus $G(t)$ satisfy

$$s\bar{J}(s) = \frac{1}{s\bar{G}(s)}, \quad \bar{G}(s) = \frac{\int_0^1 \phi_\epsilon(\alpha)s^\alpha d\alpha}{s\int_0^1 \phi_\sigma(\alpha)s^\alpha d\alpha}. \tag{7}$$

With the creep compliance $J(t)$ and the relaxation modulus $G(t)$, the strain response and stress response are

$$\epsilon(t) = J(t) * \dot{\sigma}(t), \quad \sigma(t) = G(t) * \dot{\epsilon}(t), \tag{8}$$

respectively, where the convolution is defined as

$$f(t) * g(t) = \int_{0^-}^{t^+} f(t-\tau)g(\tau)d\tau. \tag{9}$$

The limiting values of the material functions for $t \to 0^+$ and $t \to +\infty$ are related to the instantaneous and equilibrium behaviors of the viscoelastic body,

Table 1. The four types of viscoelasticity.

Type	$J(0^+)$	$J(+\infty)$	$G(0^+)$	$G(+\infty)$
I	>0	$<\infty$	$<\infty$	>0
II	>0	$=\infty$	$<\infty$	$=0$
III	$=0$	$<\infty$	$=\infty$	>0
IV	$=0$	$=\infty$	$=\infty$	$=0$

respectively. It follows from the limiting theorems for the Laplace transform that

$$J(0^+) = 1/G(0^+), \quad J(+\infty) = 1/G(+\infty). \tag{10}$$

According to the instantaneous and equilibrium responses, viscoelastic bodies are classified in four types[4,7,8] as in Table 1. We note that such interesting classification was introduced in 1971 by Caputo and Maidardi.[4] The Kelvin–Voigt, the Maxwell and the Zener models are the simplest viscoelastic bodies of types III, II, I, respectively.[8]

In next section, we investigate the creep compliance, creep-recovery, relaxation modulus, energy dissipation or hysteresis under periodic deformation, etc., by using the distributed order constitutive equation for two cases of the constitutive functions. We express these responses and results as easily computable forms and simulate them by using MATHEMATICA 8.

2. Response Analysis and Simulation

We consider two cases of the constitutive functions, respectively. Case A characterizes viscoelastic materials of type IV while Case B belongs to type I according to Table 1. For each case, we investigate (i) creep compliance and creep recovery, (ii) relaxation modulus, and (iii) harmonic deformation and stress–strain behavior.

Case A. $\phi_\sigma(\alpha) = \delta(\alpha)$, $\phi_\epsilon(\alpha) = E\,(\tau_0)^\alpha$, where $\delta(\alpha)$ is the Dirac delta function, E and τ_0 are positive constants.

In this case, the distributed order constitutive relation degenerates to

$$\sigma(t) = E \int_0^1 (\tau_0)^\alpha \epsilon^{(\alpha)}(t) d\alpha. \tag{11}$$

Applying the Laplace transform and then integrating with respect to α yield

$$\bar{\sigma}(s) = \frac{E\,(\tau_0 s - 1)}{\ln(\tau_0 s)} \bar{\epsilon}(s). \tag{12}$$

(i) Creep compliance and creep recovery

The Laplace transform of creep compliance $J(t)$ is

$$\bar{J}(s) = \frac{\ln(\tau_0 s)}{E\,s\,(\tau_0 s - 1)}. \tag{13}$$

From the initial value and final value theorems, we have

$$J(0^+) = \lim_{s\to\infty} s\bar{J}(s) = 0, \quad J(+\infty) = \lim_{s\to 0} s\bar{J}(s) = +\infty. \tag{14}$$

In order to express the creep compliance $J(t)$, we use the formula

$$L^{-1}\left[\frac{\ln(s+1)}{s}\right] = E_1(t), \quad \mathrm{Re}s > 0, \tag{15}$$

where $E_1(t)$ is the exponential integral function defined by

$$E_1(t) = \int_t^\infty \frac{e^{-u}}{u} du. \tag{16}$$

Hence, from the properties of Laplace transform we derive

$$L^{-1}\left[\frac{\ln(\tau_0 s)}{\tau_0 s - 1}\right] = \frac{1}{\tau_0} e^{\frac{t}{\tau_0}} E_1\left(\frac{t}{\tau_0}\right), \quad \mathrm{Re}s > \frac{1}{\tau_0}, \tag{17}$$

and the creep compliance

$$J(t) = \frac{1}{E\tau_0}\int_0^t e^{\frac{t}{\tau_0}} E_1\left(\frac{t}{\tau_0}\right) dt. \tag{18}$$

We note that the exponential integral function $E_1(t)$ is a built-in function in most computer algebra systems such as MATHEMATICA 8. In Fig. 1, creep compliance $J(t)$ for $E = 1$ and for $\tau_0 = 0.5, \tau_0 = 1$ and $\tau_0 = 2$ are shown, where the time interval is taken on $[0, 20]$ and we calculate each values for $t = 0.05k, k = 0, 1, \ldots, 400$. The continuous curves are formed by linear interpolation.

Note that no instantaneous elastic deformation is possible and the model undergoes creep indefinitely, which is a characteristic of a viscoelastic fluid.

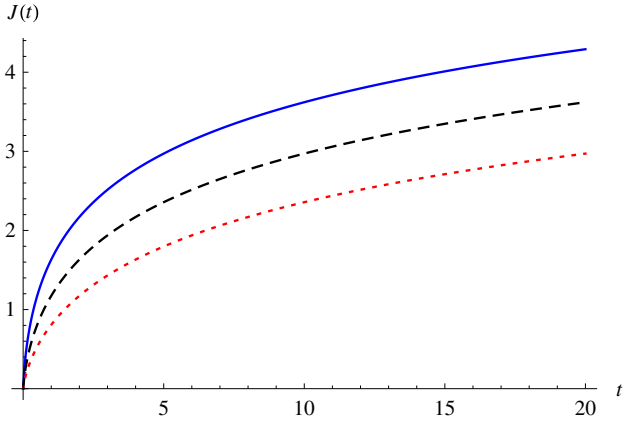

Fig. 1. Curves of creep compliance $J(t)$ for $E = 1$ and for $\tau_0 = 0.5$ (solid line), $\tau_0 = 1$ (dash line) and $\tau_0 = 2$ (dot line).

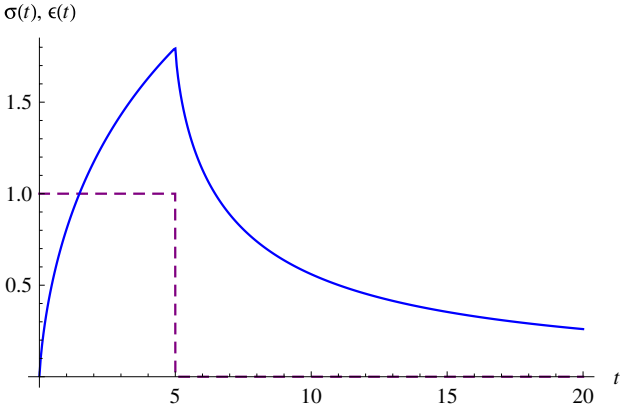

Fig. 2. Suddenly applied and then removed fixed stress $\sigma(t)$ (dash line) and the creep recovery response $\epsilon(t)$ (solid line) for $E = 1$, $\tau_0 = 2$ and $T = 5$.

To examine the creep recovery response, we remove the load suddenly. Thus, the applied stress can be expressed as $\sigma(t) = H(t) - H(t-T)$. Its Laplace transform is $\bar{\sigma}(s) = \frac{1}{s}(1 - e^{-Ts})$. We obtain the creep recovery response

$$\epsilon(t) = J(t) - J(t-T)H(t-T), \tag{19}$$

where the final value is $\epsilon(+\infty) = 0$. In Fig. 2, we display the curve of creep recovery response $\epsilon(t)$ for $E = 1$, $\tau_0 = 2$ and $T = 5$.

We note that for elastic materials, such strain recovery is instantaneous and complete. Here, the model exhibits an eventually complete creep recovery.

(ii) Relaxation modulus

The Laplace transform of relaxation modulus $G(t)$ takes the form

$$\bar{G}(s) = \frac{E(\tau_0 s - 1)}{s\ln(\tau_0 s)} = E\left(\frac{\tau_0}{\ln(\tau_0 s)} - \frac{1}{s\ln(\tau_0 s)}\right). \tag{20}$$

The initial value and final value of relaxation modulus $G(t)$ are given as

$$G(0^+) = +\infty, \quad G(+\infty) = 0.$$

In order to inverse Eq. (20), we present the Laplace inverse formula

$$L^{-1}\left[\frac{1}{\ln(s)}\right] = e^t + \int_0^{+\infty} \frac{e^{-rt}}{\ln^2(r) + \pi^2} dr. \tag{21}$$

To prove the formula (21), we start with the complex integral formula for the inverse transform (5). The function $\frac{1}{\ln(s)}$ has a pole $s = 1$, and branch points $s = 0$ and $s = \infty$, so we take the negative real axis as a cut and consider the one-valued branch satisfying $-\pi < \arg s < \pi$.

We express the Laplace inversion integral as a Hankel contour integral plus the residue at $s = 1$, i.e.,

$$L^{-1}\left[\frac{1}{\ln(s)}\right] = \frac{1}{2\pi i}\int_{\mathrm{Ha}(\varepsilon)} \frac{1}{\ln(s)} e^{st}\mathrm{d}s + \mathrm{Res}\left(\frac{1}{\ln(s)} e^{st}, s = 1\right), \tag{22}$$

where the Hankel path $\mathrm{Ha}(\varepsilon)$ denotes a counterclockwise loop constructed by a small circle $|s| = \varepsilon$ with $\varepsilon \to 0$ and by the two sides of the negative real axis.

Decomposing the integral by substituting $s = re^{\pm i\pi}$ along the upper and lower sides of the cut and $s = \varepsilon e^{i\theta}$ along the small circle $|s| = \varepsilon$ and calculating the residue, we have

$$L^{-1}\left[\frac{1}{\ln(s)}\right] = \frac{1}{2\pi i}\left[\int_0^{\infty}\left(\frac{1}{\ln(r) - i\pi} - \frac{1}{\ln(r) + i\pi}\right)e^{-rt}dr + \lim_{\varepsilon\to 0^+}\int_{-\pi}^{\pi}\frac{i\varepsilon e^{i\theta}e^{\varepsilon t e^{i\theta}}}{\ln(\varepsilon) + i\theta}\,\mathrm{d}\theta\right] + e^t.$$

The limitation vanishes so we obtain the formula in Eq. (21).

Utilizing properties of Laplace transform, we further obtain

$$L^{-1}\left[\frac{1}{\ln(\tau_0 s)}\right] = \frac{1}{\tau_0}\left[e^{\frac{t}{\tau_0}} + \int_0^{+\infty}\frac{e^{-rt/\tau_0}}{\ln^2(r) + \pi^2}dr\right], \tag{23}$$

and

$$L^{-1}\left[\frac{1}{s\ln(\tau_0 s)}\right] = e^{\frac{t}{\tau_0}} - 1 + \int_0^{+\infty}\frac{1 - e^{-rt/\tau_0}}{r(\ln^2(r) + \pi^2)}dr. \tag{24}$$

From Eqs. (20), (23) and (24), we derive the relaxation modulus as

$$G(t) = E\left[1 + \int_0^{+\infty}\frac{(r+1)e^{-rt/\tau_0} - 1}{r(\ln^2(r) + \pi^2)}dr\right], \quad t > 0, \tag{25}$$

or more concisely as

$$G(t) = E\int_0^{+\infty}\frac{(r+1)e^{-rt/\tau_0}}{r(\ln^2(r) + \pi^2)}dr, \quad t > 0. \tag{26}$$

We note that the integral in Eq. (26) is divergent if $t = 0$, which verifies the initial value $G(0^+) = +\infty$. In Fig. 3. We plot the curves of the relaxation modulus $G(t)$ versus t for $E = 1$ and for $\tau_0 = 0.5, 1$ and 2, where the values of $G(t)$ are calculated at $t = 0.001 + 0.05k$ for $k = 0, 1, \ldots, 400$ and interpolated linearly.

Note that the stress relaxes out completely over time, which is a characteristic of a viscoelastic fluid.

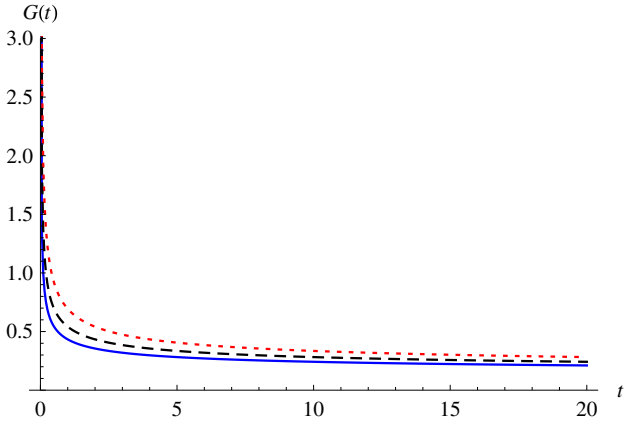

Fig. 3. Curves of the relaxation modulus $G(t)$ versus t for $E = 1$ and different values of τ_0: $\tau_0 = 0.5$ (solid line), $\tau_0 = 1$ (dash line) and $\tau_0 = 2$ (dot line).

(iii) Harmonic deformation and stress–strain behavior

If strain is of harmonic deformation $\epsilon(t) = \sin(2\pi t)$, we use formulas (8), (26) and

$$e^{at} * \cos(bt) = \frac{ae^{at} - a\cos(bt) + b\sin(bt)}{a^2 + b^2} H(t), \tag{27}$$

and obtain the stress response

$$\begin{aligned}\sigma(t) &= 2\pi G(t) * \cos(2\pi t) \\ &= 2\pi E\tau_0 \int_0^{+\infty} \frac{(r+1)(r\cos(2\pi t) + 2\pi\tau_0 \sin(2\pi t) - re^{-\frac{rt}{\tau_0}})}{r(r^2 + 4\pi^2\tau_0^2)(\ln^2(r) + \pi^2)} dr. \end{aligned} \tag{28}$$

It is readily to find out the initial value $\sigma(0^+) = 0$ and asymptotic periodic behavior

$$\sigma(t) \sim 2\pi E\tau_0(C_1\cos(2\pi t) + C_2\sin(2\pi t)), \quad t \to +\infty, \tag{29}$$

where C_1 and C_2 are constants

$$C_1 = \int_0^{+\infty} \frac{(r+1)}{(r^2 + 4\pi^2\tau_0^2)(\ln^2(r) + \pi^2)} dr,$$

$$C_2 = \int_0^{+\infty} \frac{2\pi\tau_0(r+1)}{r(r^2 + 4\pi^2\tau_0^2)(\ln^2(r) + \pi^2)} dr.$$

In Fig. 4, curves of stress response $\sigma(t)$ versus t are shown for $E = 1$ and $\tau_0 = 0.5, 2, 4$, respectively. The values of $\sigma(t)$ are calculated at $t = 0.005k$ for $k = 0, 1, \ldots, 1000$ and interpolated linearly. Phase difference between stress and strain is obvious, which means hysteresis and energy dissipation. In Fig. 5, stress–strain hysteresis loop for $E = 1$ and $\tau_0 = 2$ is shown by using the same data as in Fig. 4. Stress response rapidly approaches a steady state. We note that since $\dot{\sigma}(0^+) = +\infty$, the value of $\sigma(0.005)$ changes obviously from the value $\sigma(0) = 0$.

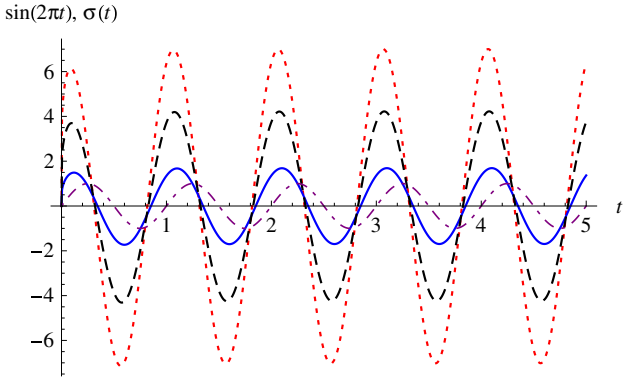

Fig. 4. Curves of $\sin(2\pi t)$ (dot-dash line) and stress response $\sigma(t)$ for $E = 1$ and $\tau_0 = 0.5$ (solid line), $\tau_0 = 2$ (dash line) and $\tau_0 = 4$ (dot line).

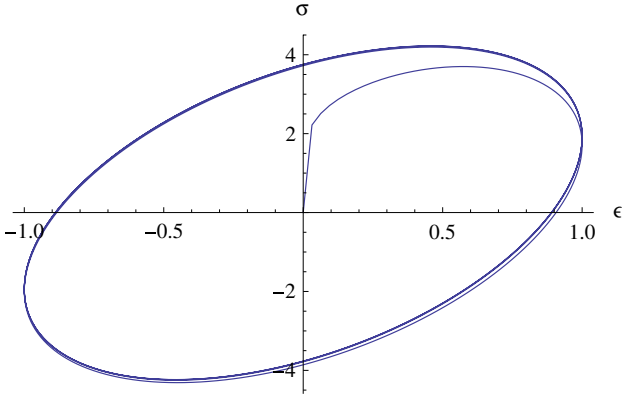

Fig. 5. Stress–strain hysteresis loop for $E = 1$ and $\tau_0 = 2$.

Any materials that exhibit hysteresis, creep or stress relaxation can be considered viscoelastic materials. In comparison, elastic materials do not exhibit energy dissipation or hysteresis as their loading and unloading curve is the same.

We note that the constitutive equation (11) characterizes viscoelastic materials of type IV according to Table 1. Such viscoelastic materials exhibit a complete stress relaxation and an infinite strain creep. They do not present equilibrium elasticity or instantaneous elasticity.

Case B. $\phi_\sigma(\alpha) = (\tau_\sigma)^\alpha$, $\phi_\epsilon(\alpha) = E\,(\tau_\epsilon)^\alpha$, where $E, \tau_\sigma, \tau_\epsilon$ are positive constants satisfying $\tau_\sigma < \tau_\epsilon$.

The inequality $\tau_\sigma < \tau_\epsilon$ follows from the second law of thermodynamics.[27,31] In this case, the distributed order constitutive relation degenerates to

$$\int_0^1 (\tau_\sigma)^\alpha \sigma^{(\alpha)}(t) d\alpha = E \int_0^1 (\tau_\epsilon)^\alpha \epsilon^{(\alpha)}(t) d\alpha. \tag{30}$$

Applying the Laplace transform and then integrating with respect to α yield

$$\bar{\sigma}(s) = \frac{E\,(\tau_\epsilon s - 1)\ln(\tau_\sigma s)}{(\tau_\sigma s - 1)\ln(\tau_\epsilon s)}\,\bar{\epsilon}(s). \tag{31}$$

(i) Creep compliance and creep recovery

Laplace transform of creep compliance $J(t)$ satisfies

$$\bar{J}(s) = \frac{(\tau_\sigma s - 1)\ln(\tau_\epsilon s)}{Es(\tau_\epsilon s - 1)\ln(\tau_\sigma s)}. \tag{32}$$

By the limiting theorem, we have the limiting values

$$J(0^+) = \frac{\tau_\sigma}{E\tau_\epsilon}, \quad J(+\infty) = \frac{1}{E}, \tag{33}$$

two positive finite values which are different from that in Case A.

To inverse Eq. (32), we make the decomposition

$$\frac{\tau_\sigma s - 1}{s(\tau_\epsilon s - 1)} = \frac{1}{s} + \frac{\tau_\sigma - \tau_\epsilon}{\tau_\epsilon s - 1}, \quad \frac{\ln(\tau_\epsilon s)}{\ln(\tau_\sigma s)} = 1 + \frac{\ln(\frac{\tau_\epsilon}{\tau_\sigma})}{\ln(\tau_\sigma s)}.$$

Then inverse transform for Eq. (32) yields

$$J(t) = \frac{1}{E}\left(H(t) + \left(\frac{\tau_\sigma}{\tau_\epsilon} - 1\right)e^{\frac{t}{\tau_\epsilon}}\right) * \left(\delta(t) + \ln\left(\frac{\tau_\epsilon}{\tau_\sigma}\right)\,L^{-1}\left[\frac{1}{\ln(\tau_\sigma s)}\right]\right).$$

Utilizing formula (23) and calculating convolution with respect to t we obtain the creep compliance

$$\begin{aligned} J(t) = {} & \frac{1}{E}\left[H(t) + \left(\frac{\tau_\sigma}{\tau_\epsilon} + \ln\left(\frac{\tau_\epsilon}{\tau_\sigma}\right) - 1\right)e^{\frac{t}{\tau_\epsilon}}\right] \\ & + \frac{1}{E}\ln\left(\frac{\tau_\epsilon}{\tau_\sigma}\right)\int_0^{+\infty} \frac{r(\tau_\sigma - \tau_\epsilon)e^{\frac{t}{\tau_\epsilon}} - \tau_\sigma(1+r)e^{-\frac{rt}{\tau_\sigma}}}{r(r\tau_\epsilon + \tau_\sigma)(\ln^2(r) + \pi^2)}dr. \end{aligned} \tag{34}$$

Taking $t = 0$ in Eq. (34), we have the same initial value as in Eq. (33). In Fig. 6, curves of creep compliance $J(t)$ versus t for $E = 1$ and different values of τ_σ and τ_ϵ are shown, where the values of $J(t)$ are calculated at $t = 0.05k$ for $k = 0, 1, \ldots, 300$, and interpolated linearly. Note that the model allows an instantaneous deformation to occur, and overtime the displacement creeps to an asymptotic level.

The creep recovery response to the stress input $\sigma(t) = H(t) - H(t - T)$ is $\epsilon(t) = J(t) - J(t - T)H(t - T)$. In Fig. 7, we plot the creep recovery response $\epsilon(t)$ for $E = 1$, $\tau_\sigma = 2$, $\tau_\epsilon = 8$ and $T = 4$. The model allows an instantaneous elastic deformation, but does not allow for a permanent strain.

(ii) Relaxation modulus

The Laplace transform of relaxation modulus $G(t)$ reads

$$\bar{G}(s) = \frac{E(\tau_\epsilon s - 1)\ln(\tau_\sigma s)}{s(\tau_\sigma s - 1)\ln(\tau_\epsilon s)}. \tag{35}$$

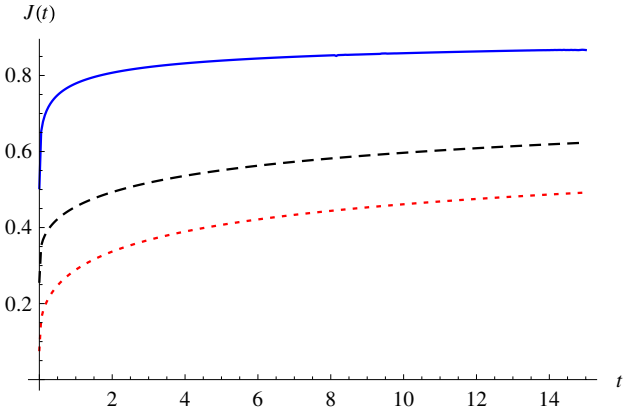

Fig. 6. Curves of creep compliance $J(t)$ versus t for $E = 1$ and $\tau_\sigma = 0.25$, $\tau_\epsilon = 0.5$ (solid line), $\tau_\sigma = 2, \tau_\epsilon = 8$ (dash line) and $\tau_\sigma = 0.25, \tau_\epsilon = 4$ (dot line).

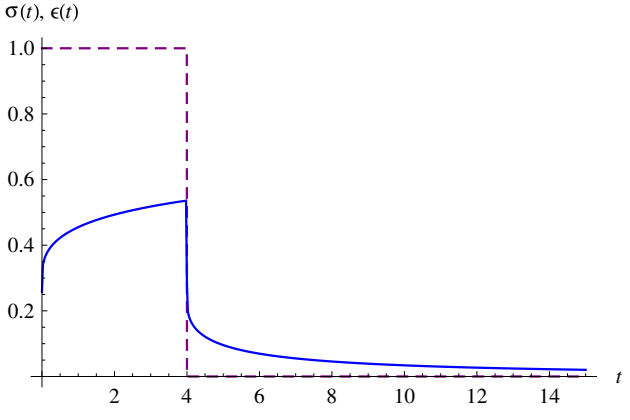

Fig. 7. Suddenly applied and then removed fixed stress $\sigma(t)$ (dash line) and the creep recovery response $\epsilon(t)$ (solid line) for $E = 1, \tau_\sigma = 2, \tau_\epsilon = 8$ and $T = 4$.

So relaxation modulus $G(t)$ is obtained by replacing E by $1/E$ and the interchange of τ_ϵ and τ_σ in Eq. (34),

$$G(t) = E\left[H(t) + \left(\frac{\tau_\epsilon}{\tau_\sigma} + \ln\left(\frac{\tau_\sigma}{\tau_\epsilon}\right) - 1\right) e^{\frac{t}{\tau_\sigma}}\right] + E\ln\left(\frac{\tau_\sigma}{\tau_\epsilon}\right)\int_0^{+\infty} \frac{r(\tau_\epsilon - \tau_\sigma)e^{\frac{t}{\tau_\sigma}} - \tau_\epsilon(1+r)e^{-\frac{rt}{\tau_\epsilon}}}{r(r\tau_\sigma + \tau_\epsilon)(\ln^2(r) + \pi^2)} dr. \tag{36}$$

Its initial and final values are $G(0^+) = \frac{E\tau_\epsilon}{\tau_\sigma}$ and $G(+\infty) = E$, two positive finite values. In Fig. 8, curves of relaxation modulus $G(t)$ versus t for $E = 1$ and different values of τ_σ and τ_ϵ are shown, where the values of $G(t)$ are calculated at $t = 0.025k$

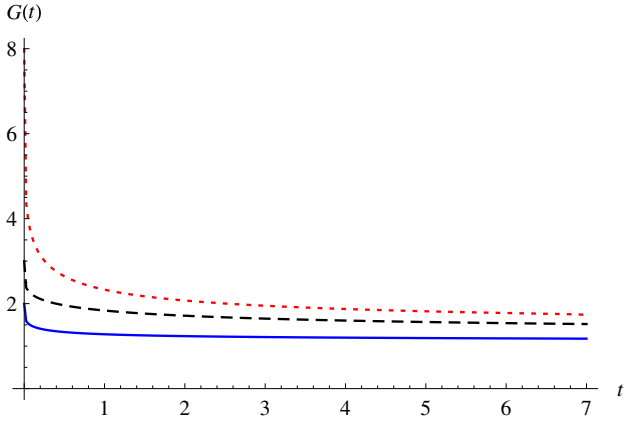

Fig. 8. Curves of relaxation modulus $G(t)$ versus t for $E = 1$ and $\tau_\sigma = 0.25$, $\tau_\epsilon = 0.5$ (solid line), $\tau_\sigma = 2, \tau_\epsilon = 6$ (dash line) and $\tau_\sigma = 0.25, \tau_\epsilon = 2$ (dot line).

for $k = 0, 1, \ldots, 280$, and interpolated linearly. Note that the stress relaxes from a finite value and approaches to a nonzero value, which is different from Case A.

(iii) Harmonic deformation and stress–strain behavior

The stress response to the harmonic deformation $\epsilon(t) = \sin(2\pi t)$ is $\sigma(t) = G(t) * 2\pi\cos(2\pi t)$, where $G(t)$ is given by Eq. (36). Here, we use the composite trapezoidal rule to calculate the convolution integral for each fixed value of t.

Suppose an equal step-size partition for variable t: $t_n = nh, n = 0, 1, \ldots, N$. Then the convolution integral is calculated numerically as $\sigma(t_0) = 0$, and

$$\begin{aligned}\sigma(t_n) &= 2\pi \int_0^{t_n} G(\tau)\cos(2\pi(t_n - \tau))d\tau \\ &= 2\pi \sum_{i=0}^{n} \omega_{n,i} G(t_i)\cos(2\pi t_{n-i}), \quad n = 1, 2, \ldots, N, \end{aligned} \tag{37}$$

where $G(t_i)$ is computed by using Eq. (36) and the weights $\omega_{n,i}$ are given as

$$\omega_{n,0} = \omega_{n,n} = h/2, \quad \omega_{n,i} = h, \quad i = 1, 2, \ldots, n-1. \tag{38}$$

In Fig. 9, we plot the curves of strain $\epsilon(t) = \sin(2\pi t)$ and the stress response $\sigma(t)$ for $E = 1$ $\tau_\sigma = 2$ and $\tau_\epsilon = 6$ on interval $0 \le t \le 5$, where the stress response $\sigma(t)$ is computed with the step-size $h = 0.0025$ and the continuous curve is generated by linear interpolation on the numerical results. In Fig. 10, stress–strain hysteresis loop is shown, where the stress rapidly approaches a steady state oscillation.

We note that the model (30) characterizes the viscoelastic material of type I according to Table 1. It exhibits both instantaneous and equilibrium elasticity, so their behavior appears close to the purely elastic one for sufficiently short and long times.

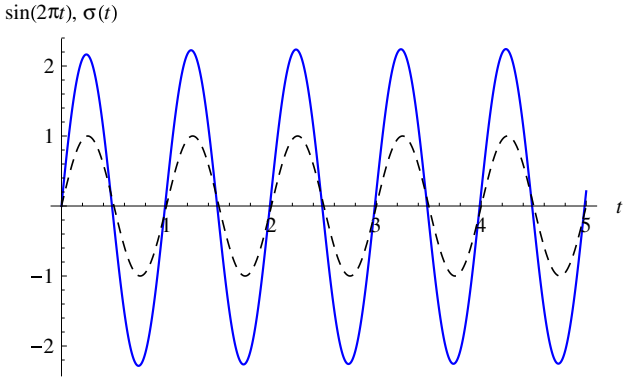

Fig. 9. Curves of strain $\sin(2\pi t)$ (dash line) and the stress response $\sigma(t)$ for $E = 1\tau_\sigma = 2$ and $\tau_\epsilon = 6$ (solid line).

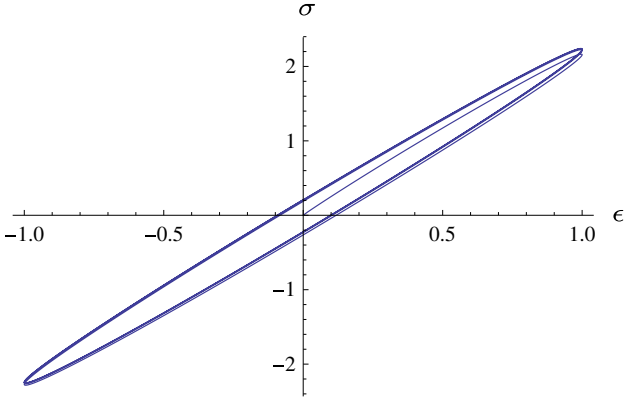

Fig. 10. Stress–strain hysteresis loop for $E = 1, \tau_\sigma = 2$ and $\tau_\epsilon = 6$.

3. Conclusions

In this paper, we investigate the response and its modeling for the distributed order constitutive equations

$$\sigma(t) = E \int_0^1 (\tau_0)^\alpha \epsilon^{(\alpha)}(t) d\alpha$$

and

$$\int_0^1 (\tau_\sigma)^\alpha \sigma^{(\alpha)}(t) d\alpha = E \int_0^1 (\tau_\epsilon)^\alpha \epsilon^{(\alpha)}(t) d\alpha,$$

respectively, where E, τ_0, τ_σ and τ_ϵ are positive constants satisfying $\tau_\sigma < \tau_\epsilon$.

For each case, we consider the creep compliance, creep recovery, relaxation modulus, stress–strain behavior under harmonic deformation. We express these responses and results as easily computable forms and simulate them by using

MATHEMATICA 8. In order to achieve our results, we present a Laplace inverse formula

$$L^{-1}\left[\frac{1}{\ln(s)}\right] = e^t + \int_0^{+\infty} \frac{e^{-rt}}{\ln^2(r) + \pi^2} dr.$$

For the first constitutive equation, we derive the creep compliance in terms of the exponential integral function, the relaxation modulus and stress response to harmonic deformation as convergent improper integrals on the infinite interval $(0, +\infty)$. For the second constitutive equation, we derive the creep compliance and the relaxation modulus as convergent improper integrals on the infinite interval $(0, +\infty)$. We obtain the stress response to harmonic deformation by using the numerical integral method for the convolution integral. For both equations, stress responses to harmonic deformation display hysteresis phenomena and energy dissipation.

The first constitutive equation characterizes viscoelastic materials of type IV while the second constitutive equation models viscoelastic materials of type I according to Table 1. The viscoelastic model of type IV is fluid-like whereas model of type I is solid-like.

All the figures are generated by using MATHEMATICA 8 based on our results. Figure 1 is generated directly by using the exponential integral function. For the other figures, we use the built-in command 'NIntegrate' in MATHEMATICA 8 to calculate the improper integrals on the interval $(0, +\infty)$ numerically. There are no other errors in the formation of Figs. 2–8. In Figs. 9 and 10, the composite trapezoidal rule to calculate the convolution integral is used. So the figures are accurate enough and we do not have to resort to numerical Laplace inverse transformation. To offer a continuous representation, we use linear interpolation on our discrete numerical results.

Acknowledgments

This work was supported by the Natural Science Foundation of Shanghai (No. 14ZR1440800) and the Course Construction Project of Shanghai Municipal Education Commission (No. 33210M161020).

References

1. Scott-Blair G. W., Analytical and integrative aspects of the stress–strain–time problem, *J. Sci. Instrum.* **21**:80–84, 1944.
2. Scott-Blair G. W., *Survey of General and Applied Rheology*, Pitman, London, 1949.
3. Gerasimov A. N., A generalization of linear laws of deformation and its application to inner friction problems, *Prikl. Mat. Mekh.* **12**:251–259, 1948.
4. Caputo M., Mainardi F., Linear models of dissipation in anelastic solids, *Riv. Nuovo Cimento* **1**:161–198, 1971.
5. Koeller R. C., Applications of fractional calculus to the theory of viscoelasticity, *J. Appl. Mech.* **51**:299–307, 1984.

6. Podlubny I., *Fractional Differential Equations*, Academic, San Diego, 1999.
7. Mainardi F., *Fractional Calculus and Waves in Linear Viscoelasticity*, Imperial College, London, 2010.
8. Mainardi F., Spada G., Creep, relaxation and viscosity properties for basic fractional models in rheology, *Eur. Phys. J. Spec. Top.* **193**:133–160, 2011.
9. Chen Y., Moore K. L., Analytical stability bound for a class of delayed fractional-Order dynamic systems, *Nonlinear Dyn.* **29**:191–200, 2002.
10. Monje C. A., Chen Y. Q., Vinagre B. M., Xue D., Feliu V., *Fractional-Order Systems and Controls, Fundamentals and Applications*, Springer, London, 2010.
11. Xu M. Y., Tan W. C., Representation of the constitutive equation of viscoelastic materials by the generalized fractional element networks and its generalized solutions, *Sci. China Ser. G* **46**:145–157, 2003.
12. Chen W., An intuitive study of fractional derivative modeling and fractional quantum in soft matter, *J. Vib. Control* **14**:1651–1657, 2008.
13. Kilbas A. A., Srivastava H. M., Trujillo J. J., *Theory and Applications of Fractional Differential Equations*, Elsevier, Amsterdam, 2006.
14. Tavazoei M. S., Haeri M., Jafari S., Bolouki S., Siami M., Some applications of fractional calculus in suppression of chaotic oscillations, *IEEE T. Ind. Electron.* **55**:4094–4101, 2008.
15. Tavazoei M. S., Haeri M., Attari M., Bolouki S., Siami M., More details on analysis of fractional-order Van der Pol oscillator, *J. Vib. Control* **15**:803–819, 2009.
16. Băleanu D., Diethelm K., Scalas E., Trujillo J. J., *Fractional Calculus Models and Numerical Methods–Series on Complexity, Nonlinearity and Chaos*, World Scientific, Boston, 2012.
17. Rogers L., Operators and fractional derivatives for viscoelastic constitutive equations, *J. Rheol.* **27**:351–372, 1983.
18. Bagley R. L., Torvik P. J., A theoretical basis for the application of fractional calculus to viscoelasticity, *J. Rheol.* **27**:201–210, 1983.
19. Schiessel H., Metzler R., Blumen A., Nonnenmacher T. F., Generalized viscoelastic models: Their fractional equations with solutions, *J. Phys. A: Math. Gen.* **28**:6567–6584, 1995.
20. Pritz T., Analysis of four-parameter fractional derivative model of real solid materials, *J. Sound Vibr.* **195**:103–115, 1996.
21. Bland D. R., *The Theory of Linear Viscoelasticity*, Pergamon, Oxford, 1960.
22. Duan J. S., Qiu X., The periodic solution of Stokes' second problem for viscoelastic fluids as characterized by a fractional constitutive equation, *J. Non-Newton. Fluid Mech.* **205**:11–15, 2014.
23. Bagley R. L., Torvik P. J., On the existence of the order domain and the solution of distributed order equations–Part I, *Int. J. Appl. Math.* **2**:865–882, 2000.
24. Bagley R. L., Torvik P. J., On the existence of the order domain and the solution of distributed order equations–Part II, *Int. J. Appl. Math.* **2**:965–987, 2000.
25. Caputo M., Distributed order differential equations modelling dielectric induction and diffusion, *Frac. Calc. Appl. Anal.* **4**:421–442, 2001.
26. Atanackovic T. M., A generalized model for the uniaxial isothermal deformation of a viscoelastic body, *Acta Mech.* **159**:77–86, 2002.
27. Atanackovic T. M., On a distributed derivative model of a viscoelastic body, *C. R. Mecanique* **331**:687–692, 2003.
28. Li Y., Sheng H., Chen Y. Q., On distributed order integrator/differentiator, *Signal Process.* **91**:1079–1084, 2011.

29. Jiao Z., Chen Y., Podlubny I., *Distributed-Order Dynamic Systems–Stability, Simulation, Applications and Perspectives*, Springer, London, 2012.
30. Sheng H., Chen Y., Qiu T., *Fractional Processes and Fractional-Order Signal Processing–Techniques and Applications*, Springer, London, 2012.
31. Bagley R. L., Torvik P. J., On the fractional calculus model of viscoelastic behavior, *J. Rheol.* **30**:133–155, 1986.